# Electronic Supplementary Information (ESI) for the article, “Structures, Electron Density and Characterization of Novel Photocatalysts, $(BaTaO_2N)_{1-x}(SrWO_2N)_x$ Solid Solutions”

Keisuke Hibino, Masatomo Yashima,* Takayoshi Oshima, Kotaro Fujii, Kazuhiko Maeda

Department of Chemistry, School of Science, Tokyo Institute of Technology, 2-2-1-W4-17, O-okayama, Meguro-ku, Tokyo, 152-8551, Japan

* Corresponding author

## Electronic Supplementary Information A: Color change of samples in ammonolysis

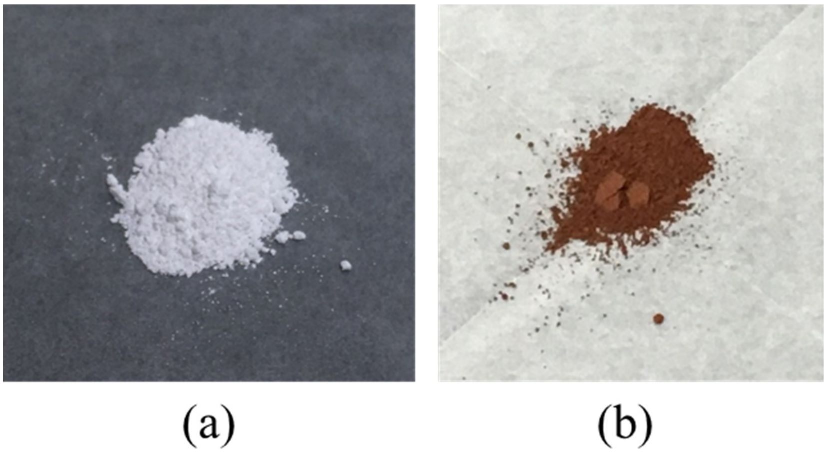
(a) (b)

**Photo 1**: Photos of (a) oxide precursor for $(BaTaO_2N)_{0.99}(SrWO_2N)_{0.01}$ and (b) oxynitride $(BaTaO_2N)_{0.99}(SrWO_2N)_{0.01}$. (a) The oxide precursor was white, while (b) the oxynitride was brown. The color change between insulating oxide precursor and semiconducting oxynitride corresponds to change in UV-Vis spectra (Fig. 7).

# Electronic Supplementary Information B: Experimental details of photocatalytic activity measurements

To investigate the photocatalytic activities of $(BaTaO_2N)_{1-x}(SrWO_2N)_x$ ($x$ = 0, 0.01, and 0.02), colloidal $IrO_2$ was loaded on $(BaTaO_2N)_{1-x}(SrWO_2N)_x$. A colloidal $IrO_2$ solution was prepared by hydrolysis of $Na_2IrCl_6$.[S1] First, $Na_2IrCl_6$ (16 mg) was dissolved in $H_2O$ (50 mL), and aqueous NaOH solution was added until the solution pH was 12. The solution was heated at 348 K for 30 min, and cooled to room temperature in an ice-water bath. Aqueous $HNO_3$ solution was then dropped slowly into the cooled solution until it reached pH 9, followed by heating 348 K for 30 min again. The obtained deep-blue solution of colloidal $IrO_2$ was diluted to a total volume of 50 mL. $(BaTaO_2N)_{1-x}(SrWO_2N)_x$ powders (0.13 g) were dispersed in $H_2O$ (25 mL) and the as-prepared colloidal $IrO_2$ solution (0.5 wt% with respect to catalyst mass) was added. The suspension was agitated for 1 h at room temperature and centrifuged to collect residual solids. The samples obtained, $IrO_2$-loaded $(BaTaO_2N)_{1-x}(SrWO_2N)_x$, were oven-dried at 343 K overnight.

Photocatalytic reactions were carried out in a Pyrex top-irradiation vessel connected to a glass closed gas circulation system. In the vessel, $IrO_2$-loaded $(BaTaO_2N)_{1-x}(SrWO_2N)_x$ photocatalyst powder (100mg) and $La_2O_3$ (100 mg) were dispersed in water (150 mL), and $AgNO_3$ (1.5 mmol) was added. Air in the solution was removed by several evacuations and Ar gas (approx. 5 kPa) was introduced into the reaction system before conducting photocatalytic reaction. Subsequently, the vessel was irradiated under visible light. The light source was a 300-W xenon lamp, and the light wavelength was controlled to be over 420 nm using a combination of a cold mirror (CM1), cut-off filter (L-42), and water filter. The reactant solution was maintained at room temperature using a water bath during reactions. Evolved gas was analyzed by gas chromatography (GL Sciences Inc., GC-3200-SYG with TDC detector, argon carrier gas).

## References

[S1] A. Harriman, I. J. Pickering, J. M. Thomas, P. A. Christensen, *J. Chem. Soc. Faraday Trans. 1 Phys. Chem. Condens. Phases*, 1988, **84**, 2795–2806.

# Electronic Supplementary Information C: Refined crystallographic parameters and reliability factors for synchrotron X-ray diffraction data of $(BaTaO_2N)_{1-x}(SrWO_2N)_x$ ($x$ = 0, 0.01, and 0.02). Composition $x$ dependence of lattice parameters of $(BaTaO_2N)_{1-x}(SrWO_2N)_x$.

**Table S1.** Refined crystallographic parameters and reliability factors for synchrotron X-ray diffraction data of $BaTaO_2N$ measured at 302 K.

| Atom | Site | Occupancy | Atomic coordinates | | | Isotropic atomic displacement parameter |
|---|---|---|---|---|---|---|
| | | $g$ | $x$ | $y$ | $z$ | $100U_{\mathrm{iso}}$ / Å$^2$ |
| Ba | 1*a* | 1 | 1/2 | 1/2 | 1/2 | 0.570(9) |
| Ta | 1*b* | 1 | 0 | 0 | 0 | 0.743(7) |
| O | 3*c* | 2/3 | 1/2 | 0 | 0 | 0.67(5)* |
| N | 3c | 1/3 | 1/2 | 0 | 0 | 0.67(5)* |

Crystal system: cubic, space-group type: $Pm\bar{3}m$

Wavelength: $\lambda$= 0.3997119(17) Å

*$U_{\mathrm{iso}}(\mathrm{O}) = U_{\mathrm{iso}}(\mathrm{N})$

Lattice parameters: $a = b = c = 4.11265(2)$ Å, $\alpha = \beta = \gamma = 90°$

Reliability factors: $R_{\mathrm{wp}} = 6.55\%$, $R_{\mathrm{p}} = 4.43\%$, $R_{\mathrm{B}} = 1.86\%$, $R_F = 0.83\%$.

BVS of *B*-site Ta cation was estimated to be 4.53, which agrees with the formal charge of 5.

**Table S2.** Refined crystallographic parameters and reliability factors for synchrotron X-ray diffraction data of $(BaTaO_2N)_{0.99}(SrWO_2N)_{0.01}$ measured at 302 K.

| Atom | Site | Occupancy | Atomic coordinates | | | Atomic displacement parameter |
|---|---|---|---|---|---|---|
| | | $g$ | $x$ | $y$ | $z$ | $100\ U_{\mathrm{iso}}$ / Å$^2$ |
| Ba | 1*a* | 100/101 | 1/2 | 1/2 | 1/2 | 0.549(11)[a] |
| Sr | 1*a* | 1/101 | 1/2 | 1/2 | 1/2 | 0.549(11)[a] |
| Ta | 1*b* | 100/101 | 0 | 0 | 0 | 0.703(9)[b] |
| W | 1*b* | 1/101 | 0 | 0 | 0 | 0.703(9)[b] |
| O | 3*c* | 2/3 | 1/2 | 0 | 0 | 0.63(6)[c] |
| N | 3*c* | 1/3 | 1/2 | 0 | 0 | 0.63(6)[c] |

Crystal system: cubic, space-group type: $Pm\bar{3}m$

Wavelength: $\lambda = 0.3997119(17)$ Å

[a] $U_{\mathrm{iso}}(\mathrm{Ba}) = U_{\mathrm{iso}}(\mathrm{Sr})$

[b] $U_{\mathrm{iso}}(\mathrm{Ta}) = U_{\mathrm{iso}}(\mathrm{W})$

[c] $U_{\mathrm{iso}}(\mathrm{O}) = U_{\mathrm{iso}}(\mathrm{N})$

Lattice parameters: $a = b = c = 4.11162(2)$ Å, $\alpha = \beta = \gamma = 90°$

Reliability factors: $R_{\mathrm{wp}} = 7.55\%$, $R_{\mathrm{p}} = 4.89\%$, $R_{\mathrm{B}} = 1.58\%$, $R_F = 0.78\%$

BVS of *B*-site Ta,W cations were estimated to be 4.54, which agrees with the formal charge of 5.

**Table S3.** Refined crystallographic parameters and reliability factors for synchrotron X-ray diffraction data of $(BaTaO_2N)_{0.98}(SrWO_2N)_{0.02}$ measured at 302 K.

| Atom | Site | Occupancy | Atomic coordinates | | | Atomic displacement parameter |
|---|---|---|---|---|---|---|
| | | $g$ | $x$ | $y$ | $z$ | 100 $U_{\mathrm{iso}}$ / Å$^2$ |
| Ba | 1*a* | 100/102 | 1/2 | 1/2 | 1/2 | 0.575(16)$^a$ |
| Sr | 1*a* | 2/102 | 1/2 | 1/2 | 1/2 | 0.575(16)$^a$ |
| Ta | 1*b* | 100/102 | 0 | 0 | 0 | 0.664(14)$^b$ |
| W | 1*b* | 2/102 | 0 | 0 | 0 | 0.664(14)$^b$ |
| O | 3*c* | 2/3 | 1/2 | 0 | 0 | 0.59(9)$^c$ |
| N | 3*c* | 1/3 | 1/2 | 0 | 0 | 0.59(9)$^c$ |

Crystal system: cubic, space-group type: $Pm\bar{3}m$

Wavelength: $\lambda = 0.3997119(17)$ Å

$^aU_{\mathrm{iso}}(\mathrm{Ba}) = U_{\mathrm{iso}}(\mathrm{Sr})$

$^bU_{\mathrm{iso}}(\mathrm{Ta}) = U_{\mathrm{iso}}(\mathrm{W})$

$^cU_{\mathrm{iso}}(\mathrm{O}) = U_{\mathrm{iso}}(\mathrm{N})$

Lattice parameters: $a = b = c = 4.11012(3)$ Å, $\alpha = \beta = \gamma = 90°$

Reliability factors: $R_{\mathrm{wp}} = 11.01\%$, $R_{\mathrm{p}} = 6.38\%$, $R_{\mathrm{B}} = 3.34\%$, $R_F = 1.46\%$

BVS of *B*-site Ta,W cations were estimated to be 4.55, which agrees with the formal charge of 5.

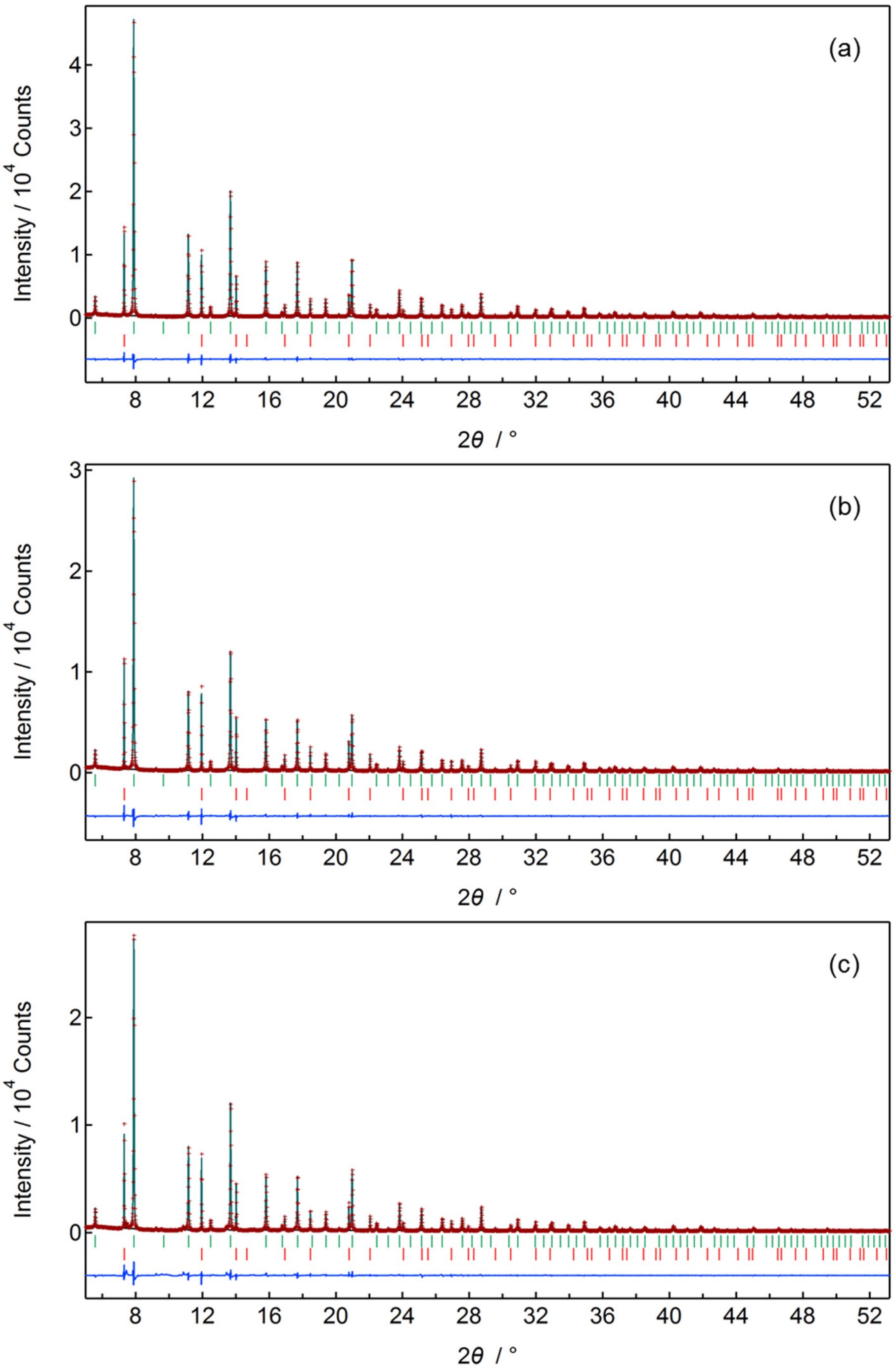

**Figure S1.** Rietveld patterns of synchrotron X-ray powder diffraction data of $(BaTaO_2N)_{1-x}(SrWO_2N)_x$ [(a) $x = 0$, (b) $x = 0.01$, and (c) $x = 0.02$] including silicon internal standard (NIST SRM640c) at 302 K. The $2\theta$ range of the analyzed data was from 3.0–53.2° and step interval of 0.01°. Brown crosses and green lines denote observed and calculated intensities, respectively. Green and red ticks represent Bragg peak positions of $(BaTaO_2N)_{1-x}(SrWO_2N)_x$ and silicon (NIST SRM640c), respectively. Blue lines at the bottom represent profile difference between observed and calculated intensities.

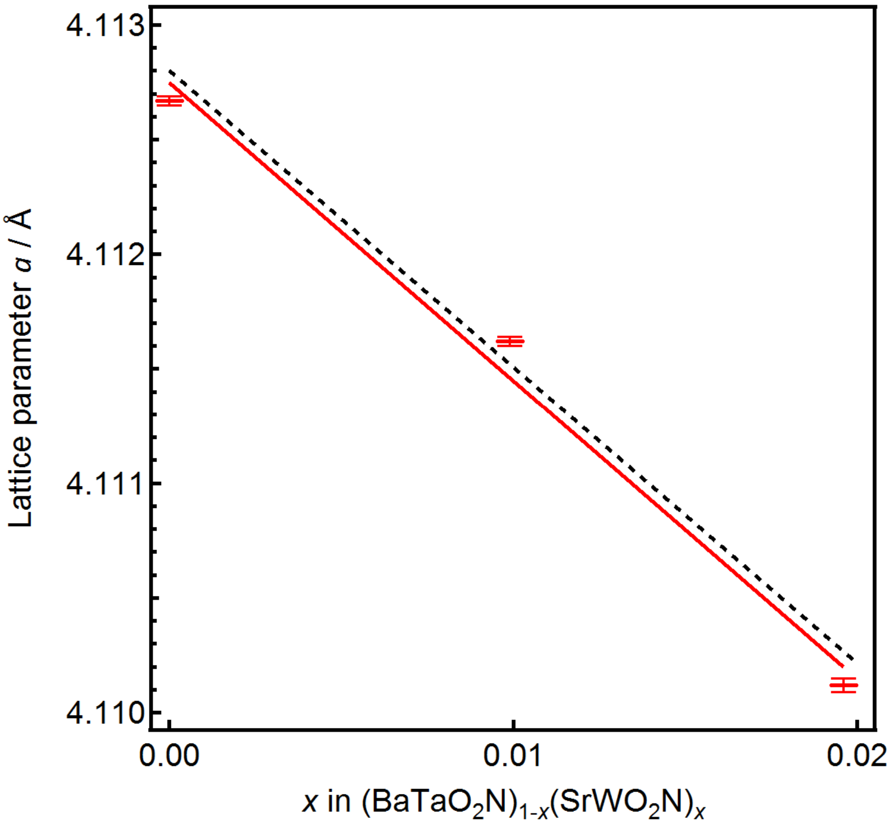

**Figure S2.** Variation in lattice parameter $a$ of $(BaTaO_2N)_{1-x}(SrWO_2N)_x$ solid solutions with $SrWO_2N$ content $x$. The red solid linear line was obtained from the least-squares fit. The black dashed line denotes calculated lattice parameter $a_{cal}(x)$, obtained using the equation $a_{cal}(x) = (1 - x)a(BaTaO_2N) + x\, a(SrWO_2N)$. Here, $a(BaTaO_2N)$ and $a(SrWO_2N)$ are the literature lattice parameters of $BaTaO_2N$ and $SrWO_2N$, respectively[S2,S3]. The results indicate that the Vegard's law is valid and that both $Ba^{2+}$ and $Ta^{5+}$ are substituted by $Sr^{2+}$ and $W^{5+}$, respectively.

## References

[S2] F. Pors, R. Marchand, Y. Laurent, P. Bacher and G. Roult, *Mater. Res. Bull.*, 1988, **23**, 1447–1450.

[S3] M. Yashima, U. Fumi, H. Nakano, K. Omoto and J. R. Hester, *J. Phys. Chem. C*, 2013, **117**, 18529–18539.

# Electronic Supplementary Information D: Estimation of band gap of $(BaTaO_2N)_{1-x}(SrWO_2N)_x$ ($x$ = 0, 0.01, and 0.02)

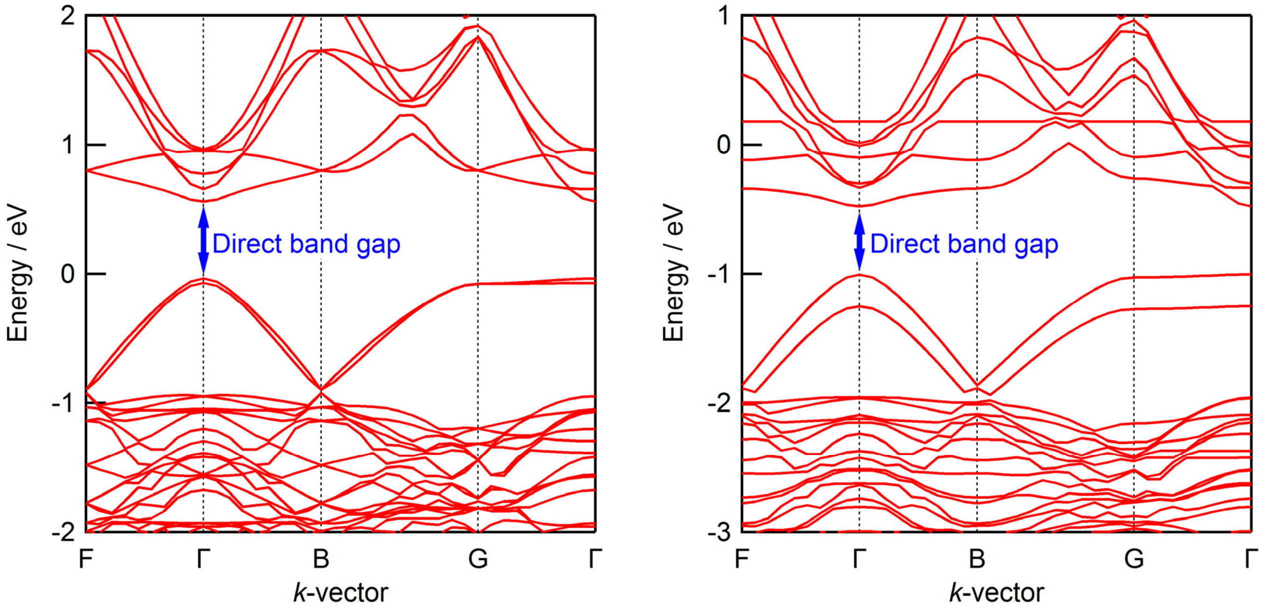

**Figure S3.** Band structures of $(BaTaO_2N)_8$ (left) and $(BaTaO_2N)_7(SrWO_2N)$ (right), which show the direct band gaps.

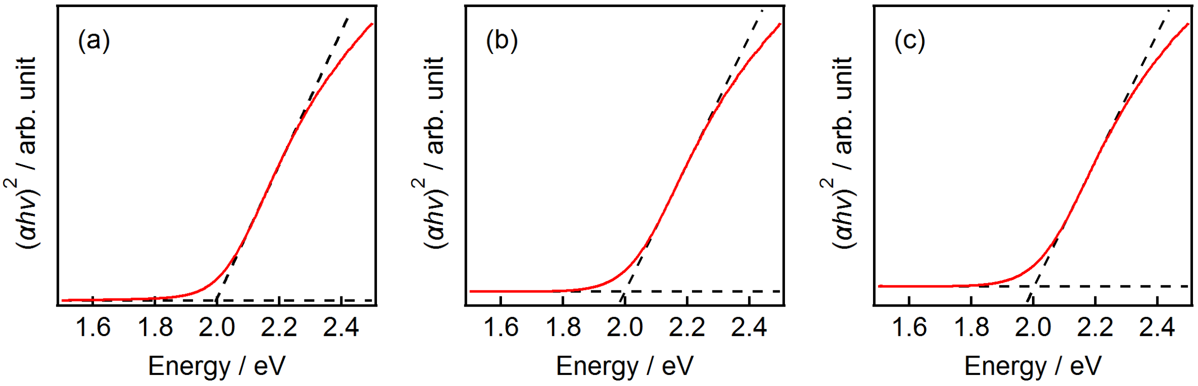

**Figure S4.** Tauc plots of $(BaTaO_2N)_{1-x}(SrWO_2N)_x$ [(a) $x = 0$, (b) $x = 0.01$, and (c) $x = 0.02$]. The absorption edge has the form $\alpha h\nu = C(h\nu - E_g)^n$, where $E_g$ is the band gap, $\alpha$ is the absorption coefficient, $h\nu$ is the photon energy, and $C$ is a constant. Here, $n$ is 1/2 because $(BaTaO_2N)_8$ and $(BaTaO_2N)_7(SrWO_2N)$ have direct band gaps (Figure S3). Estimated band gaps were 2.0 eV for all compositions of (a) $x = 0$, (b) $x = 0.01$, and (c) $x = 0.02$.

# Electronic Supplementary Information E:Photocatalytic activity results for $(BaTaO_2N)_{1-x}(SrWO_2N)_x$ ($x$ = 0 and 0.02)

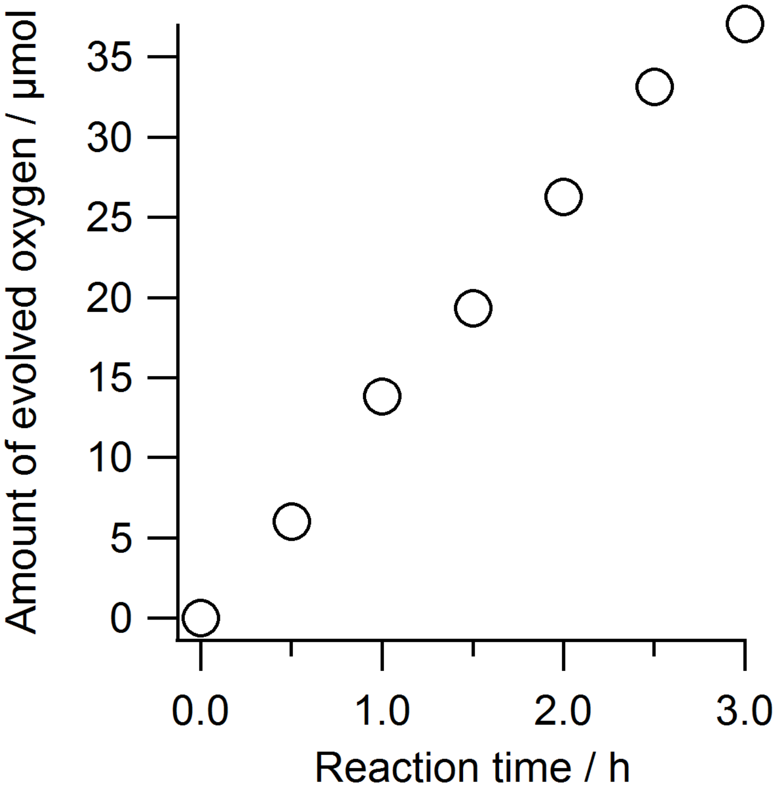

**Figure S5.** Time course of $O_2$ evolution on $BaTaO_2N$ under visible-light irradiation ($\lambda > 420$ nm) from silver nitrate solution containing of $La_2O_3$ (100 mg). Reaction conditions: 0.5 wt% $IrO_2$-loaded $BaTaO_2N$ catalyst (100 mg), aqueous silver nitrate solution (10.0 mM, 150 mL), and top-irradiation-type reaction vessel. Light source: xenon lamp (300 W) with cutoff filter.

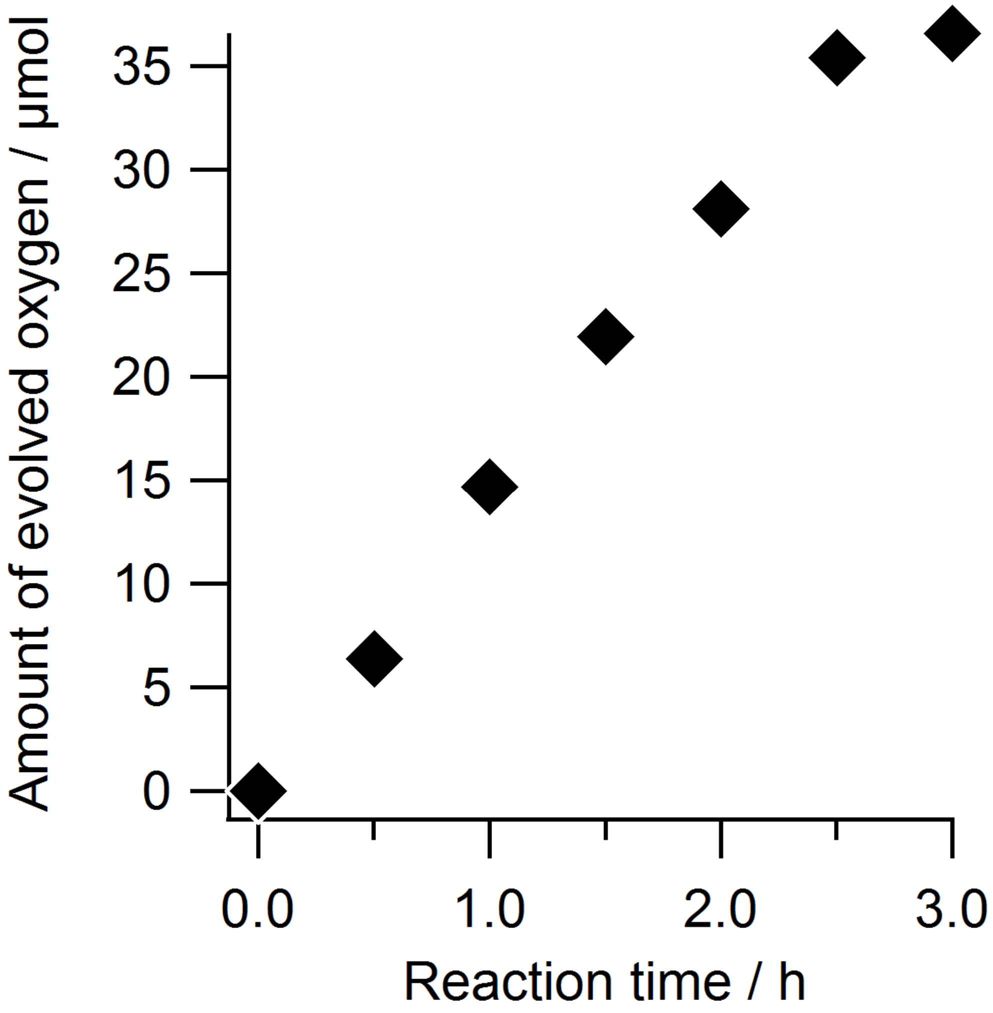

**Figure S6.** Time course of $O_2$ evolution on $(BaTaO_2N)_{0.98}(SrWO_2N)_{0.02}$ under visible-light irradiation ($\lambda > 420$ nm) from silver nitrate solution containing $La_2O_3$ (100 mg). Reaction conditions: 0.5 wt% $IrO_2$-loaded $(BaTaO_2N)_{0.98}(SrWO_2N)_{0.02}$ catalyst (100 mg), aqueous silver nitrate solution (10.0 mM, 150 mL), and top-irradiation-type reaction vessel. Light source: xenon lamp (300 W) with cutoff filter.

## End of the Electronic Supplementary Information